A high-throughput pipeline to determine DNA and nucleosome conformations by AFM imaging

Sebastian Konrad, Willem Vanderlinden, Jan Lipfert

Angaben zur Veröffentlichung / Publication details:

Konrad, Sebastian, Willem Vanderlinden, and Jan Lipfert. 2021. "A high-throughput pipeline to determine DNA and nucleosome conformations by AFM imaging." Bio-protocol 11 (19): e4180. https://doi.org/10.21769/bioprotoc.4180.

Please cite this article as: Konrad, S. F. *et al.* (2021). A High-throughput Pipeline to Determine DNA and Nucleosome Conformations by AFM Imaging. *Bio-protocol* 11(19): e4180. DOI: 10.21769/BioProtoc.4180.

bio-protocol www.bio-protocol.org/e4180 Bio-protocol 11(19): e4180. DOI:10.21769/BioProtoc.4180

A High-throughput Pipeline to Determine DNA and Nucleosome Conformations by AFM Imaging

Sebastian F. Konrad, Willem Vanderlinden* and Jan Lipfert*

Department of Physics and Center for Nanoscience, LMU Munich, Amalienstr. 54, 80799 Munich, Germany

*For correspondence: willem.vanderlinden@lmu.de; jan.lipfert@lmu.de

[Abstract] Atomic force microscopy (AFM) is a powerful tool to image macromolecular complexes with nanometer resolution and exquisite single-molecule sensitivity. While AFM imaging is well-established to investigate DNA and nucleoprotein complexes, AFM studies are often limited by small datasets and manual image analysis that is slow and prone to user bias. Recently, we have shown that a combination of large scale AFM imaging and automated image analysis of nucleosomes can overcome these previous limitations of AFM nucleoprotein studies. Using our high-throughput imaging and analysis pipeline, we have resolved nucleosome wrapping intermediates with five base pair resolution and revealed how distinct nucleosome variants and environmental conditions affect the unwrapping pathways of nucleosomal DNA. Here, we provide a detailed protocol of our workflow to analyze DNA and nucleosome conformations focusing on practical aspects and experimental parameters. We expect our protocol to drastically enhance AFM analyses of DNA and nucleosomes and to be readily adaptable to a wide variety of other protein and protein-nucleic acid complexes.

Keywords: Atomic force microscopy, AFM, DNA, Nucleosome, Image analysis

[Background] Nucleosomes are the basic units of compaction of eukaryotic DNA into chromatin and function as regulators of gene readout and activity (Bowman and Poirier, 2015; Sadakierska-Chudy and Filip, 2015; Baldi *et al.*, 2020). Canonical nucleosome core particles consist of two copies each of the four histones H2A, H2B, H3, and H4 assembled into a histone octamer that is tightly wrapped by 147 bp of DNA (Luger *et al.*, 1997; Richmond and Davey, 2003). Accessibility to the genetic code for readout and processing is facilitated by (partial) unwrapping of nucleosomal DNA and can be achieved either by active processes involving, *e.g.,* RNA polymerase or nucleosome chaperones that exert forces and torques on the nucleosomes (Sirinakis *et al.*, 2011; Mueller-Planitz *et al.*, 2013; Narlikar *et al.*, 2013; Ordu *et al.*, 2016), or spontaneously by thermal fluctuations (Li and Widom, 2004). Using single-molecule micromanipulation techniques such as optical tweezers, the energetics of force-induced nucleosome unwrapping has been probed at high resolution (Mihardja *et al.*, 2006; Hall *et al.*, 2009; Schlingman *et al.*, 2014; Ngo *et al.*, 2015; Kaczmarczyk *et al.*, 2020). However, the unwrapping landscape in the absence of force has been more difficult to access.

Atomic force microscopy (AFM) is a powerful tool to probe nucleosome structure and interactions due to its capability to image molecular complexes at the single-molecule level, label-free, and with sub-nanometer resolution, well suited to visualize the DNA and protein components of nucleosomes

Please cite this article as: Konrad, S. F. *et al.* (2021). A High-throughput Pipeline to Determine DNA and Nucleosome Conformations by AFM Imaging. *Bio-protocol* 11(19): e4180. DOI: 10.21769/BioProtoc.4180.

(Shlyakhtenko *et al*., 2009; Bintu *et al*., 2011; Miyagi *et al*., 2011; Katan *et al*., 2015; Ordu *et al*., 2016). Recent improvements in hardware make fast imaging of thousands of molecules possible, and combination with automated image analysis enables highly quantitative and reproducible studies of DNA and nucleoprotein complexes (Dufrêne *et al*., 2017; Ando, 2018; Brouns *et al*., 2018; Würtz *et al*., 2019; Bangalore *et al*., 2020).

By combining large field of view AFM imaging and automated image analysis of DNA and nucleosomes, we have recently elucidated the nucleosomal wrapping landscape for passive invasion of nucleosomes with linker DNA, in contrast to the previous force-induced unwrapping assays (Konrad *et al*., 2021). While we have demonstrated the strength of our methodology by quantitatively capturing the conformational ensemble of wild-type and CENP-A nucleosomes – centromeric nucleosomes where histone H3 is replaced with the CENP-A variant – the methodology can be easily adapted to study a wide range of open questions such as the effect of post-translational modifications on nucleosome wrapping or the impact of DNA sequence on nucleosome positioning on the single-molecule level.

The current protocol describes all steps necessary to study DNA and nucleosomes by AFM imaging, starting with the surface deposition of the molecules and ending with the quantitative image analysis after AFM imaging. The protocol describes AFM imaging of dry samples in air. However, it can be readily adapted for AFM measurements in liquid. In liquid, the deposition protocol and imaging parameters have to be adjusted. In particular, instead of drying the surface after depositing the sample, the sample buffer solution remains on the surface for imaging. Examples of how to perform liquid AFM measurements have been published previously (Bussiek *et al*., 2003; Brouns *et al*., 2018). Subsequent analysis of the AFM images might also require adjustment of the image analysis parameters (see AFM image analysis).

Materials and Reagents

A. For surface deposition of the sample
   1. Mica Grade V-1 25 mm discs (SPI Supplies, catalog number: 01926-MB)
   2. Marking tape ROTI (Carl Roth, catalog number: 8000.1)
   3. 50 ml irrigation syringes (Braun, catalog number: 4617509F)
   4. Parafilm (Carl Roth, catalog number: H666.1)
   5. Protein LoBind Tubes 0.5 ml (Eppendorf, catalog number: 0030108094)
   6. Petri dishes (Carl Roth, catalog number: 0690.1)
   7. Kimwipes (Kimtech, catalog number: 5511)
   8. Milli-Q H_2O (Merck, catalog number: Z00Q0V0WW)
   9. Poly-L-lysine (Sigma Aldrich, catalog number: P0879 – diluted to 0.01% in Milli-Q H_2O)
   10. N_2 gas (to blow dry the surface)
   11. DNA/nucleosome sample – prepared as described previously (Krietenstein *et al*., 2012)
   12. Ethanol (Carl Roth, catalog number: T171.4 – diluted to 80% with Milli-Q water)
   13. Deposition buffer (see Recipes)

B. For AFM imaging
   1. Glass slides (Thermo Scientific Menzel, catalog number: 15998086)
   2. Double-sided adhesive discs (SPI Supplies, catalog number: 05095-AB)

Equipment

1. Self-closing tweezers (SPI Supplies, catalog number: SN5AP-XD)
2. Vortex mixer (Scientific Industries, catalog number: SU-0236)
3. Centrifuge (to fit 0.5 ml Eppendorf tubes and spin down tube content; Carl Roth, catalog number: T464.1)
4. Tweezers ESD-safe (SPI Supplies, catalog number: 0CFT07PE-XD)
5. AFM cantilevers for high-speed imaging in air; we used FASTSCAN-A (resonance frequency 1400 kHz, spring constant 18 N/m; Bruker) or AC160TS (200-400 kHz, 26 N/m; Olympus) cantilevers
6. Imaging AFM; we employed a Nanowizard Ultra Speed 2 (Bruker) and a MultiMode 8 (Bruker)

Software

1. Software to plane-correct the raw AFM data (see section “AFM image analysis”)
2. Microsoft Excel
3. Python 3
4. Software toolbox to analyze DNA and nucleosomes in AFM images (previously described in Konrad *et al.*, 2021), and available for download at https://github.com/SKonrad-Science/AFM_nucleoprotein_readout)

Procedure

A. Surface deposition of the sample

Note: Contamination can affect the quality of the imaging surface and thus imaging quality in general. It is therefore important that all instruments are kept clean throughout the process.

1. Clean the workbench with ethanol and kimwipes thoroughly. Flush the tip of the self-closing tweezers with ethanol and blow-dry the tweezers with N_2 gas. Place the tweezers on a kimwipe such that the tip does not get contaminated and does not touch the bench (Figure 1A).

Please cite this article as: Konrad, S. F. *et al.* (2021). A High-throughput Pipeline to Determine DNA and Nucleosome Conformations by AFM Imaging. *Bio-protocol* 11(19): e4180. DOI: 10.21769/BioProtoc.4180.

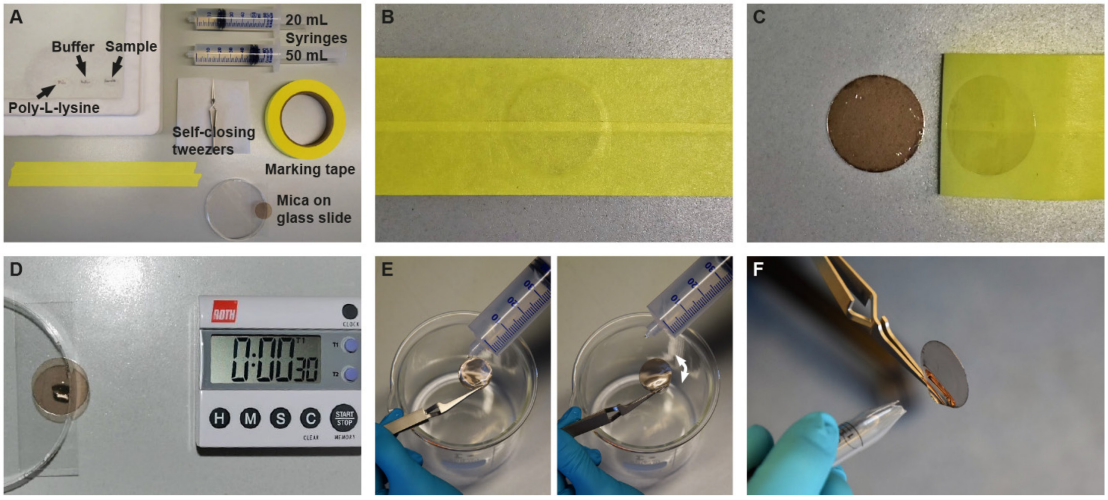

Figure 1. Surface deposition steps. A. Overview of materials required for the surface deposition of the sample as described in Materials and Reagents. **B.** A mica disc is placed under marking tape. **C.** Tearing off the tape removes a layer of the mica plate and leaves behind a flat and clean surface for the subsequent sample deposition. **D.** Poly-L-lysine and sample solutions are pipetted on the center of the mica plate and incubated for 30 s each, with washing and drying steps **E** and **F** directly after each incubation. **E.** After 30 s of incubation, the surface is rinsed by gently dropping 50/20 ml Milli-Q H_2O of the syringes on the surface and letting it flow off by rotating the mica plate. **F.** After rinsing, the surface is dried by perpendicularly pointing a nozzle with a gentle stream of N_2 gas onto the surface.

2. Place two stripes of the marking tape next to each other on the bench with a small overlap (Figure 1A) such that they are wide enough to completely cover the mica disc. Tear off part of the marking tape and put the mica disc underneath. Apply pressure such that the tape fully attaches to the surface of the mica (Figure 1B). Tear off the tape with a quick movement to cleave the mica (Figure 1C). It is important that a full layer of the mica is removed. If only part of a layer was removed or if there are small cracks on the remaining surface, repeat this step until a whole layer is removed. Store the cleaved mica disc in a Petri dish while preparing the next steps.
3. Remove two sterile syringes from their packing and remove the plunger. Make sure that the front of the plunger and the syringe barrel do not make contact anywhere to avoid contamination. Seal the syringe barrels with the clean side of parafilm and fill with Milli-Q water. Place the plunger back in the barrel and press down the plunger such that the parafilm tears and water flows out of the syringes. Remove the parafilm and adjust the plunger such that one syringe holds 50 ml and the other syringe holds 20 ml of Milli-Q water. Filling the syringes directly from the storage bottle from the back, as opposed to drawing up fluid with the plunger, helps to avoid contaminations.

4. Prepare a 20 µl aliquot of the 0.01% poly-L-lysine (see Materials and Reagents), shortly vortex it, and briefly spin down the content of the Eppendorf tube in a centrifuge (~2 s at 700 rcf). Keep the aliquot on ice.
5. Pipette the 20 µl poly-L-lysine solution onto the center of the freshly cleaved mica (step 2) and incubate for 30 s (Figure 1D). Make sure not to touch the surface with the pipette. During the 30 s incubation, pick up the mica plate with the self-closing tweezers and pick up the 50 ml syringe and move to a sink or a waste container to be able to start flushing after exactly 30 s. It is important to keep the mica surface horizontal and as still as possible during the movements to ensure a high quality of the surface deposition. Flush the surface by dropping droplets from the syringe on the edge of the mica plate (not in the center where the poly-L-lysine was placed) and periodically tilting the mica plate such that the water flows off (Figure 1E). After flushing with 50 ml, make sure to leave some water on the surface to avoid unintentional drying.
6. With the surface still covered in water, start drying the mica surface with a gentle stream of N_2 gas by quickly tilting the mica surface to a vertical position and targeting the center of the mica with the stream perpendicularly, at about 2 cm distance (Figure 1F). Once the center of the surface is dry, move the stream to the edges until the mica is completely dry.
7. Dilute the sample solution with buffer (in our case, 200 mM NaCl + 10 mM Tris) to achieve the desired concentration for surface deposition and incubate on ice for 60 s. Nucleosome samples and buffer are stored at 4°C and put on ice before starting the surface deposition. A total volume of at least 25 µl is required for surface deposition. We typically dilute 1 µl nucleosome/DNA sample solution (containing roughly 30 ng/µl 486 bp DNA and 10 ng/µl histones, corresponding to ~120 nM nucleosomes; prepared as described in Krietenstein *et al.*, 2012) with 40 µl buffer solution resulted in a good surface density for AFM imaging (*i.e.*, dense enough to have many molecules in one field of view but not too dense to have too many molecules overlap with each other).
8. After 60 s of incubation on ice, pipette 25 µl of the buffered sample solution on the center of the poly-L-lysine coated mica plate and incubate for 30 s. Again, proceed as in steps 5 and 6, rinsing – this time with a 20 ml volume of Milli-Q water – and subsequently drying the surface.
9. Store the mica disc in the Petri dish at room temperature until starting the AFM measurement. The AFM surface should always be prepared on the measurement day.

B. AFM imaging of nucleosomes and DNA

Note: The imaging is performed on a Nanowizard Ultraspeed 2 system, and the steps presented here will slightly vary for other instruments. The steps to start the measurement are only briefly described since they can be found in the user manual of the respective AFM system in detail. The focus of this section lies on tips and tricks on how to tune AFM imaging and what to look out for to achieve the highest image quality for large datasets of DNA and nucleosomes.

1. To prepare the final imaging surface, place three double-sided adhesive discs on a glass slide while leaving an area in the center free (Figure 2A). Place the sample mica plate on the adhesive

Please cite this article as: Konrad, S. F. *et al.* (2021). A High-throughput Pipeline to Determine DNA and Nucleosome Conformations by AFM Imaging. *Bio-protocol* 11(19): e4180. DOI: 10.21769/BioProtoc.4180.

region such that the central area of the mica aligns with the adhesive-free region of the glass slide and apply gentle pressure on the mica above the three adhesive discs, *i.e.*, not in the center where the sample was placed, with the tweezers to fixate the mica more strongly.

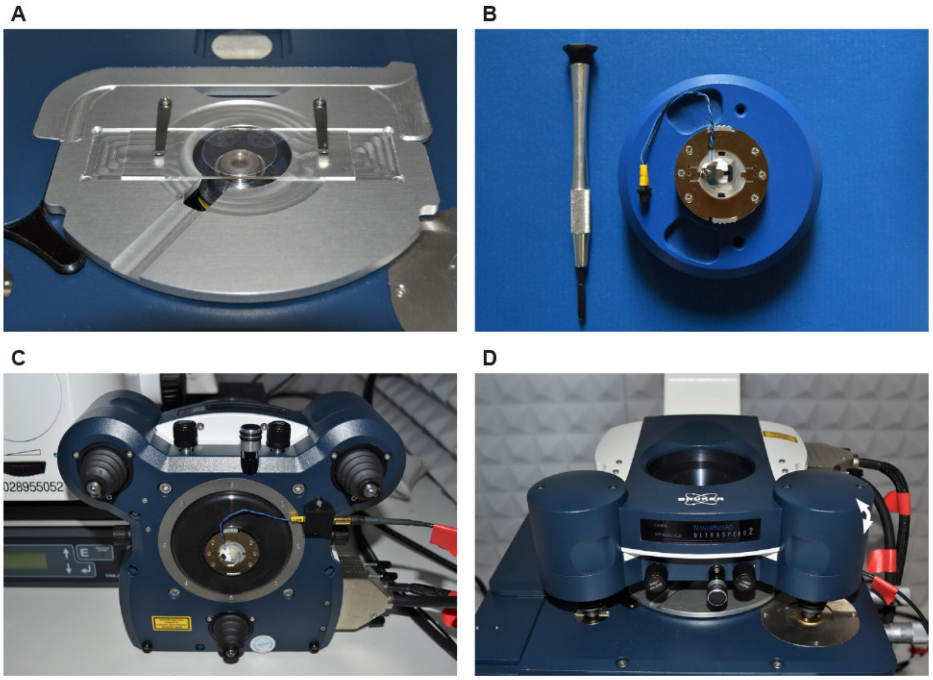

Figure 2. Mounting the sample in the AFM. A. The mica plate with the deposited sample is fixated on a glass slide with three double-sided adhesive discs. The glass side is then placed on the AFM stage. **B.** The AFM cantilever is mounted onto the glass block that was delivered with the AFM system (Ultra-Speed Glassblock, JPK, catalog number: 22229-E-01). **C.** Subsequently, the glass block is placed in the designated spot at the bottom of the AFM scanner head. **D.** To finalize the setup, the scanner head is placed on the AFM stage.

2. Install the glass slide with the mica plate on the sample holder of the AFM (Figure 2A).
3. Place the cantilever in the cantilever holder glass block (Figure 2B) and mount the glass block in the AFM scanner head (Figure 2C). Afterwards, place the AFM head on the stage (Figure 2D).

   Start the *JPK SPM Desktop* software and select *AC Mode Fast Imaging* (Figure 3A).

Please cite this article as: Konrad, S. F. *et al.* (2021). A High-throughput Pipeline to Determine DNA and Nucleosome Conformations by AFM Imaging. *Bio-protocol* 11(19): e4180. DOI: 10.21769/BioProtoc.4180.

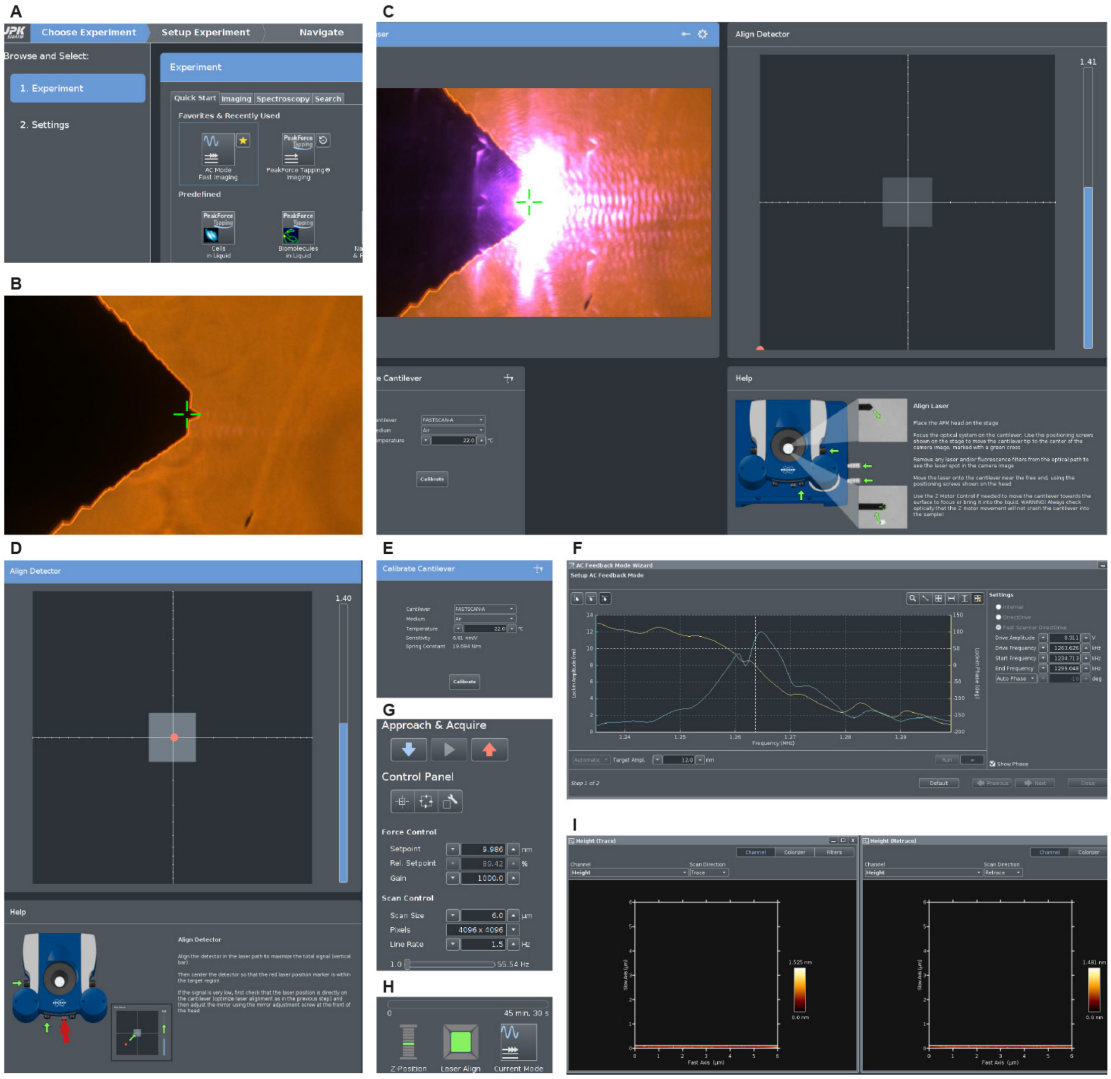

Figure 3. AFM software and settings for imaging. A. The *JPK SPM Desktop* (7.0.128) software has several imaging modes available. The desired mode for this experiment is *AC Mode Fast Imaging*. **B.** Via an optical microscope, a view of the AFM cantilever allows to place the cantilever centrally within the scanner head (green cross). **C.** Laser alignment onto the tip of the cantilever to maximize the amount of signal reflected towards the detector. **D.** Alignment of the detector such that the maximum of the signal is in the center of the quadrant detector. **E.** Cantilever calibration based on the thermal noise spectrum yields an estimated spring constant of 19.7 N/m. **F.** *AC Feedback Mode Wizard* to select the drive frequency and the drive amplitude of the AFM cantilever. **G.** Typical imaging settings used for our DNA and nucleosome images. **H.** System status after successful approach of the cantilever towards the surface. **I.** Scanning of the first lines of a 6 µm × 6 µm field of view displaying both image trace (left) and retrace (right).

4. Go to the “Setup Experiment” tab and focus the green crosshair on the AFM cantilever tip as seen in the camera view (Figure 3B).

5. Align the laser on the cantilever tip using the screws indicated by the green arrows in Figure 3C to maximize the signal that is collected by the detector. The sum of the collected signal is represented by the blue bar (Figure 3C). For FASTSCAN-A cantilevers, a sum signal between 1.3 and 1.5 is typical. Other cantilevers yield different sum signals based on the reflection achieved by the back of the cantilever tip.
6. Align the detector such that the maximum of the signal is in the center of the quadrant detector using the screws marked by the green arrows in Figure 3D. In case that proper alignment of the laser is not possible, adjust the mirror that reflects the laser signal towards the detector first (red arrow Figure 3D), and then do alignment fine-tuning with the screws afterwards.
7. To calibrate the cantilever, select the room temperature and press on “calibrate” (Figure 3E). The calibration uses the thermal noise spectrum (Mullin and Hobbs, 2014) of the cantilever and determines the spring constant and the inverse lever sensitivity, which is used to convert the measured cantilever deflection from V to nm. The spring constant should lie within the specifications of the cantilevers used (for FASTSCAN-A cantilevers typically between 17-19 N/m but may vary for different batches).
8. Go to the “Acquire data” tab and scan the cantilever for its resonance frequency in the *AC Feedback Mode Wizard* (Figure 3F). For FASTSCAN-A cantilevers, it should be around 1.2-1.4 MHz. Select the driving frequency for the measurement by placing the horizontal dashed line (Figure 3F) slightly left of the peak. Place the horizontal dashed line accordingly to reach a setpoint of 85-90% at a target amplitude of 12 nm.
9. Start approaching the surface by pressing the “Approach” button (Figure 3G). It is recommended to coarse approach the surface with the head internal Z scanner as it covers a larger Z range and switch to the smaller but faster “Fast HG” scanner before starting to scan (this can be done in the *Z Scanner Selection* menu). Our typical imaging parameters are shown under *Force Control* and *Scan Control* (Figure 3G). After the approach succeeded, the *z-position* and the *Laser Align* should be in green color (Figure 3H).
10. Once approached to the surface, verify the resonance peak again in the *AC Feedback Mode Wizard* window, as the cantilever resonance can change under the influence of a nearby surface.
11. Start imaging (Figure 3I).

    Notes: Choose image size, scan speed, and pixels once and keep the settings constant. In our experience, the best results were obtained at a resolution of 1.46 nm/pixel either scanning 2,048 × 2,048 pixels in a 3 µm × 3 µm field of view or scanning 4,096 × 4,096 pixels in a 6 µm × 6 µm field of view. Scanning is then performed at 3 or 1.5 lines per second, respectively. The image size represents a compromise between the number of molecules imaged and the imaging time required. The field of view should not be smaller than 3 µm × 3 µm since it is important to have enough molecules (>100 DNA and nucleosomes) for good statistics in the subsequent analysis. Conversely, when scanning even larger areas (e.g., 12 µm × 12 µm), the time required for recording one image at scanning speeds low enough to enable excellent resolution starts to

exceed 1 h, such that cantilever wear and drift become problematic. In addition, very large images are computationally cumbersome to process.

a. *Scanning speed matters! When scanning too fast, the molecules will appear less "sharp" and thus image quality will overall be worse. However, scanning too slowly will increase the effect of drift on the image. The scanning speed chosen should thus be as high as possible while maintaining the sharp imaging of molecules. For this purpose, we usually measure the diameter of DNA on the surface as it appears in the AFM image. Due to tip convolution, the DNA does not have a visible diameter of 2 nm, as expected from its crystal structure. A 6-8 nm DNA apparent full width at half maximum is a good value to target for ongoing AFM imaging making sure that the molecular resolution is high enough for quantitative assessment of the structural parameters. Sometimes, achieving a stable 6-8 nm DNA diameter can be difficult and requires tuning of the imaging parameters (i.e., adapting the drive frequency, the drive amplitude, the setpoint, and feedback gain) or exchanging the cantilever.*

b. *For the large images with hundreds of molecules imaged here, nonlinear behavior and hysteresis of the piezos can cause artifacts and distortions that affect the structural parameters of DNA and nucleosomes. As an example, when imaging 3 µm × 3 µm images on a MultiMode8 AFM (Bruker), DNA molecules appear shorter in the beginning (bottom) of the scan than at the end (top of the image, Figure 4A). This shortening effect is strongest for the first scans but still occurs at reduced intensity in subsequent scans. In contrast, scanning even larger 6 µm × 6 µm images on the Nanowizard Ultraspeed 2 does not show these nonlinear effects (Figure 4B). Typically, while continuously imaging, these nonlinear effects and drift tend to decrease over time once the system stabilizes after warming up.*

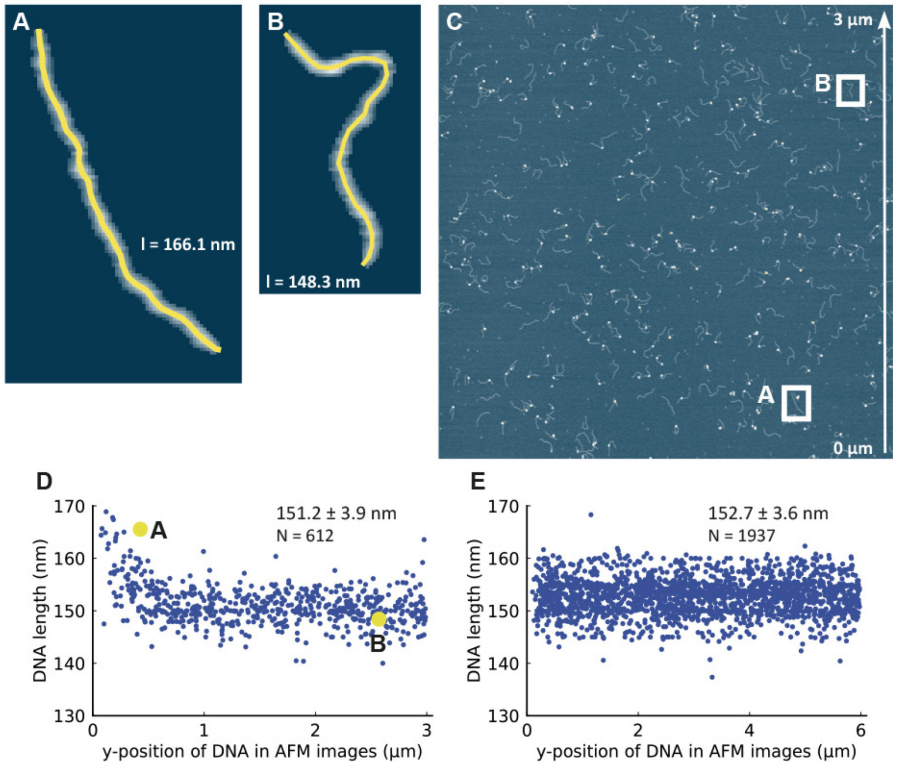

Figure 4. DNA length as a quality control parameter to detect AFM scanning artifacts. A. Example DNA strand at the bottom of an AFM image acquired on a MultiMode 8 AFM system. **B.** Example DNA strand at the top of an AFM image acquired on a MultiMode 8 AFM system. The traced DNA contour is indicated by the yellow line in A and B. **C.** AFM image with a field of view of 3 µm × 3 µm imaged at 2,048 × 2,048 pixels acquired on a MultiMode 8 AFM system. The DNA molecules shown in detail in panels A and B are indicated by the boxes in the image. **D.** Distribution of DNA lengths measured at different y-positions (bottom to top) from a total of 10 AFM images on a MultiMode 8 AFM equipped with a tube scanner. Nonlinear effects in the AFM system, likely piezo creep, cause the DNA strands in the bottom of the image to appear to have different lengths than the DNA strands elsewhere in the image. **E.** Distribution of DNA lengths measured at different y-positions (bottom to top) for the JPK Nanowizard Ultraspeed 2. For this instrument, the drift effects due to piezo creep are significantly reduced, likely due to its linearized scanner design.

c. *All AFM cantilevers are different, and important properties such as tip radius, resonance frequency, and spring constant can vary significantly between batches. Even cantilevers that are within the specifications of the respective model can show significant variations in obtainable image quality. On the Nanowizard Ultraspeed 2 AFM setup, we had the best imaging results with FASTSCAN-A cantilevers (Bruker). On a MultiMode 8 AFM system that was used in the past, we had the best imaging results using AC160TS cantilevers (Olympus). However, due to the lower resonance frequency of the AC160TS cantilevers compared to FASTSCAN-A cantilevers and due to the smaller maximum image size of the MultiMode 8*

Please cite this article as: Konrad, S. F. *et al.* (2021). A High-throughput Pipeline to Determine DNA and Nucleosome Conformations by AFM Imaging. *Bio-protocol* 11(19): e4180. DOI: 10.21769/BioProtoc.4180.

(2048^2 pixels), both the scanning speed (1 Hz) and the field of view (3 µm × 3 µm to keep the pixel size constant) are generally smaller and make the system more prone to drift and limited statistics when analyzing the image. Still, it was possible to take data sets of similar quality – despite the imaging taking longer on the MultiMode 8 – on both instruments.

C. AFM image analysis

Note: We have developed an analysis pipeline written in Python to analyze the AFM images, which has been described in detail previously (Konrad et al., 2021). A detailed guide on how to set up the Python analysis pipeline can be found via https://github.com/SKonrad-Science/AFM_nucleoprotein_readout. Therefore, the image analysis pipeline is described only briefly here, and the focus will lie on tips and tricks on how to test image quality from the structural parameters obtained from the image readout. In addition, we discuss possible further analyses to obtain additional parameters such as DNA persistence length and states of nucleosome wrapping.

1. To preprocess the raw AFM images, apply either a plane fit or an average profile fit to the surface and subsequently apply a line-wise leveling to remove observable steps between subsequent scan lines due to noise in the scanner system. The plane correction can be performed using either the image analysis software supplied by the AFM manufacturer (JPK Data Processing from JPK in our case, Figure 5A-C) or using the commercially available software SPIP (Image Metrology, Figure 5D-E). Save the leveled AFM image as an ASCII file for further processing.

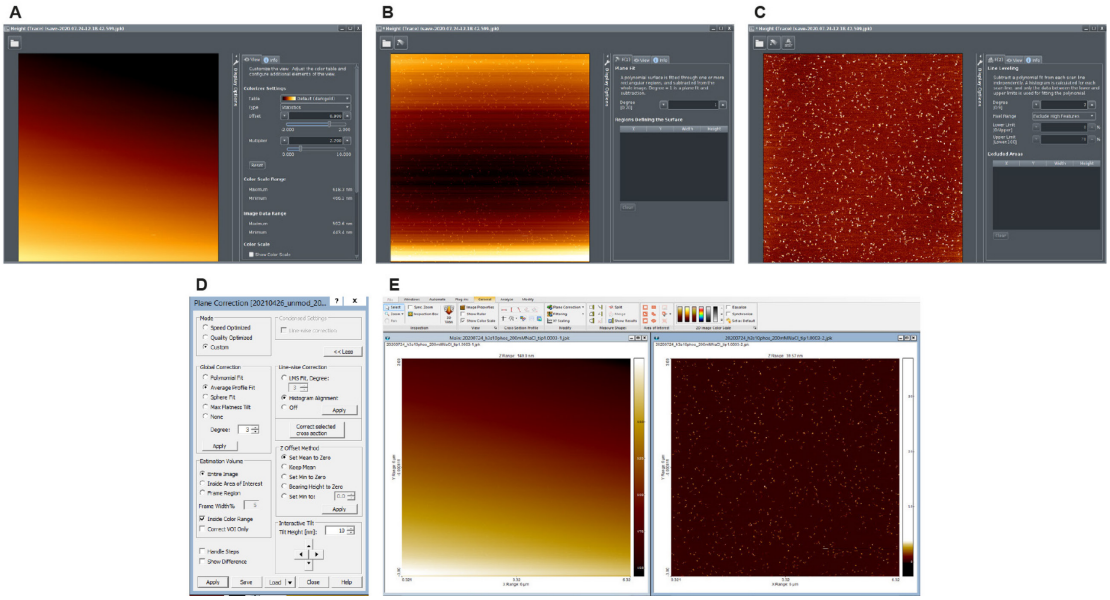

Figure 5. Plane correction of the raw AFM image. A. Raw AFM image displayed in the JPK Data Processing software (version 7.0.128). **B.** AFM image after applying a plane fit of first order. **C.** AFM image after consecutively applying line leveling. **D.** Plane correction parameters best used when plane correcting the raw AFM image using SPIP (Parameters: Mode, *Custom*; Global Correction, *Average Profile Fit*; Estimation Volume, *Entire Image*; Line-wise Correction,

Please cite this article as: Konrad, S. F. *et al.* (2021). A High-throughput Pipeline to Determine DNA and Nucleosome Conformations by AFM Imaging. *Bio-protocol* 11(19): e4180. DOI: 10.21769/BioProtoc.4180.

Histogram Alignment; and Z Offset Method, *Set Mean to Zero*). **E.** The same raw image as shown in panel A (left) and after applying the plane correction in SPIP (right).

2. Open the custom Python code as described in the installation guide (Konrad *et al.*, 2021) and select the desired analysis parameters. See Figure 6A for example analysis parameters used for analyzing the DNA and nucleosomes in our images. Depending on the background noise level, parameter tuning might be needed to maximize molecule detection. If the value of the background threshold chosen is too small, the molecules cannot be separated properly from the background, and if the value chosen is too high, the molecules might become fractured. Still, thresholding does not affect the final nucleosome parameters such as volume, opening angle, or height.
3. Run the code and select the image you want to analyze from the file dialogue (Figure 6B). DNA and nucleosomes are then detected, and their structural parameters are analyzed automatically (Figure 6C). The results are saved to an Excel worksheet. As described in the user manual, you can also choose to manually help to categorize molecules that cannot be categorized automatically (such as two slightly overlapping DNA strands) by setting the manual filtering parameter (Figure 6A) to *True*.

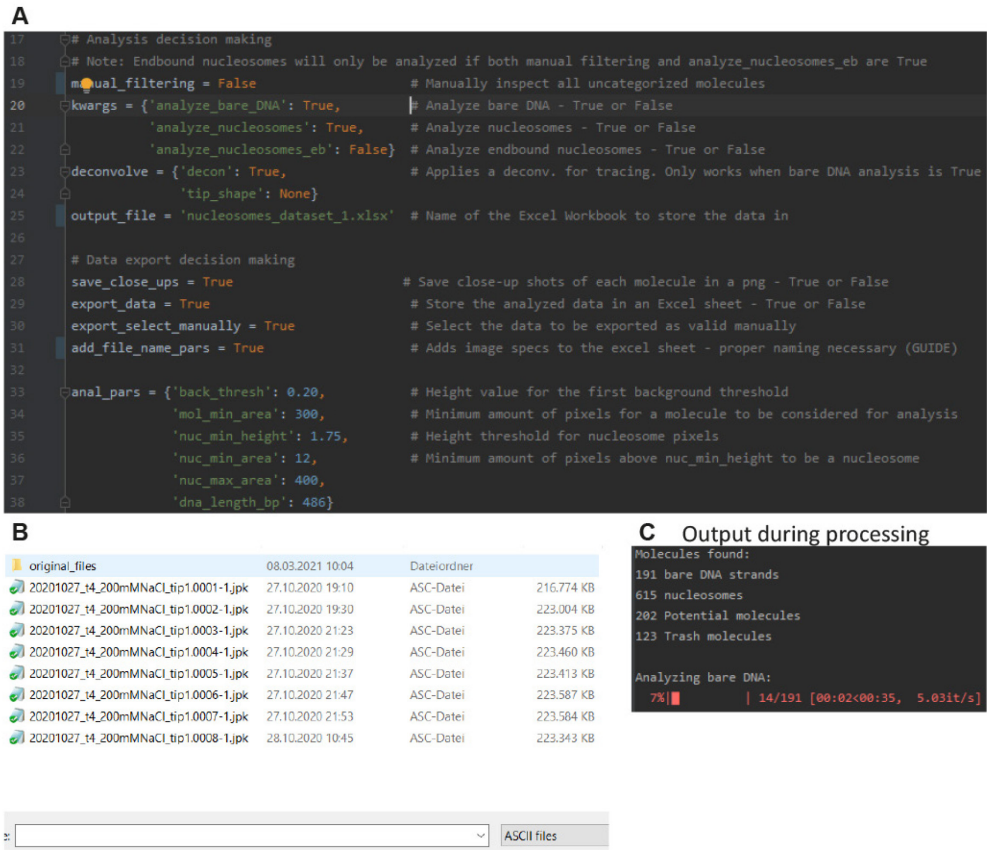

Figure 6. Image analysis post-processing software. A. Example input parameter settings for automated readout of the AFM images. **B.** File dialogue to select the desired AFM image for

automated readout. **C.** Output of the analysis software during processing. The number of molecules detected in one example AFM image.

4. Repeat the image analysis for all images of the data set to have all DNA and nucleosomes of the imaging run analyzed.
5. The structural parameters stored in the Excel worksheet can be used to gain a broad understanding of the DNA and nucleosomes in the images and serve as an input for further analysis, for example, by principal component analyses or clustering. For an example, data set of wild-type nucleosomes reconstituted on a DNA segment of 486 bp, possible further analysis and plots are shown in Figure 7A-7G.

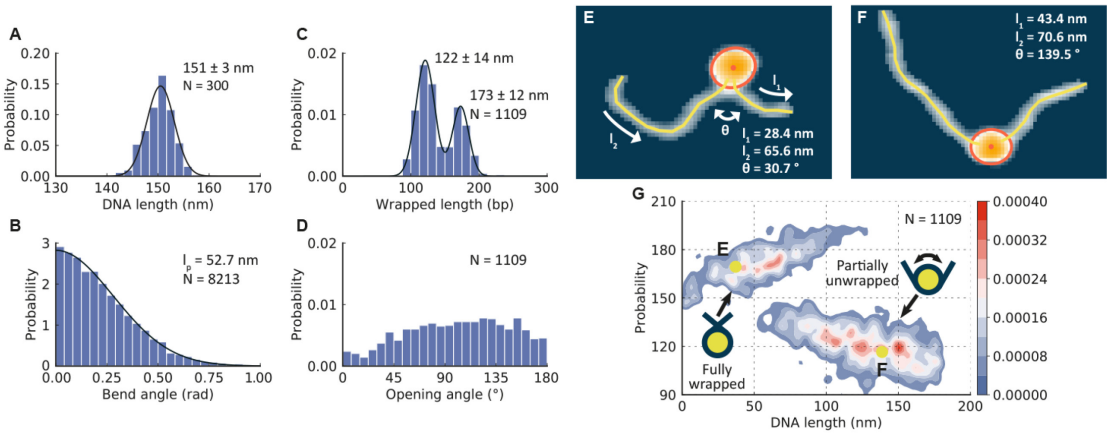

Figure 7. Example analysis of DNA and nucleosome conformations for a dataset obtained with the protocol presented here. A. Distribution of bare DNA lengths. The solid line is a Gaussian fit centered at 151 ± 3 nm (mean ± STD). **B.** The DNA length is determined by tracing its contour with segments of 5 nm length, and the relative orientation of consecutive segments yields DNA bend angles. The solid line is a fit with a folded Gaussian, as described previously (van Noort *et al*., 1999), to obtain the DNA persistence length (l_p = 52.7 nm). **C.** Distribution of DNA length wrapped around nucleosomes. The solid line is a double Gaussian fit to the data. The peaks are centered at 120 ± 14 bp and 168 ± 12 bp (mean ± STD). **D.** Distribution of nucleosome opening angles. **E.** Example image and tracing of a fully wrapped nucleosome. **F.** Example of an analyzed partially unwrapped nucleosome. **G.** 2D kernel density profile (bandwidth = 2.5°, 2.5 bp) of nucleosome opening angles and wrapped lengths. The cartoons in the insets depict the qualitative shape of fully and partially wrapped nucleosomes.

Notes:

a. *We typically deposit both bare DNA and nucleosomes on each surface for imaging since the average length of the bare DNA is used to estimate the amount of wrapped DNA of a nucleosome by subtracting the length of the two arms from the average bare DNA length. Using the DNA length determined from co-deposited molecules is more accurate than using an*

average DNA length from separate imaging runs since even if the tip geometry does not change while measuring, the bare DNA length might differ slightly between images due to changes in drift.

b. *Looking at the average values of structural parameters such as the average length of bare DNA and the average nucleosome volume provides insights into the change in data quality for a specific dataset. As a rule of thumb, for a well-imaged high-quality dataset, the average bare DNA length should not differ by more than 2 nm over multiple images. Similarly, constant average nucleosome volume (exhibiting no more than 5-10% difference for images of the same dataset) is a good measure for image quality, and an increase or, in general, variation of nucleosome volume during a measurement run indicates changes in the tip geometry and will affect the structural parameters in general (Figure 8).*

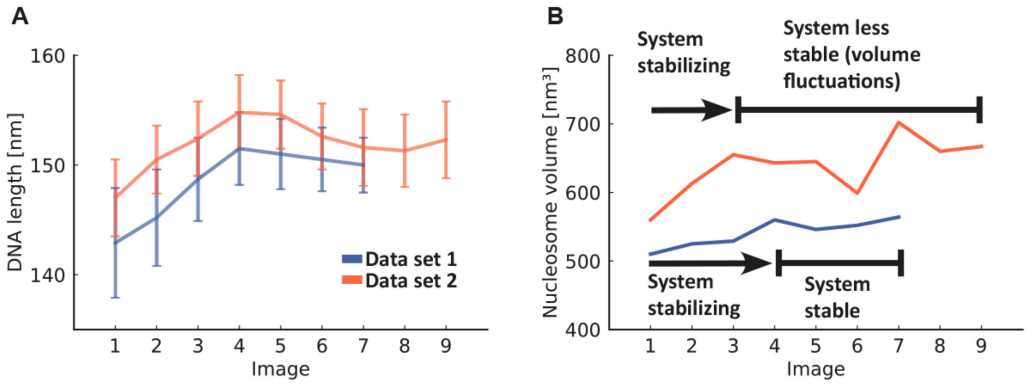

Figure 8. DNA length and nucleosome volume as quality control parameters for AFM imaging. A. Average DNA length in subsequent images (mean and standard deviation over ~200 DNA strands per image). **B.** Average nucleosome volumes in subsequent images (mean over ~400 nucleosomes per image). Shown are two data sets obtained on a Nanowizard Ultraspeed 2, each comprising multiple 6 × 6 μm^2 images. All images in one data set were obtained using the same AFM tip. Data set 1 consists of 7 AFM images, and data set 2 consists of 9 AFM images that were analyzed with respect to DNA and nucleosome structural parameters such as DNA length and nucleosome volume. For data set 1, the system stabilized during the first three images as indicated by almost constant DNA lengths and nucleosome volumes after image 3. In contrast, in data set 2, the volume parameter still shows fluctuations after several hours of imaging *(*~45 min per image), indicating that the system is less stable. Overall, in data set 2, the DNA lengths and the volumes are larger than for data set 1, indicating that the AFM cantilever has a less sharp tip.

c. *A detailed description of how to extract 5 bp unwrapping populations from the data obtained using this protocol can be found in our previous publication (Konrad et al., 2021).*

d. *Typically, datasets of ~1,000 nucleosomes or more are required to allow for a detailed analysis of the unwrapping landscape.*

e. *Additional parameters that are stored in the output Excel sheet, such as radius of gyration, end-to-end distance, or length of the individual nucleosome arms, allow for many different analyses. As an example, the 2D distribution of arm lengths and opening angles can be used to test for anti-cooperative unwrapping, or the ratio of arm lengths can be used to assess nucleosome positioning along the DNA strand.*

Notes

1. While this protocol was developed for imaging and analysis of DNA and nucleosomes, it can be readily adapted to other nucleo-protein complexes.
2. Short chained poly-L-lysine should be used to guarantee a monolayer on the surface.
3. Our surface deposition and imaging protocol is compatible with a broad range of ionic conditions. For example, we obtained high-quality images using 10 mM NaCl, 200 mM NaCl or 2 mM $MgCl_2$ (always with 10 mM TRIS, pH 7.6). Importantly, ionic conditions significantly affect DNA and nucleosome geometry (Lipfert *et al.*, 2014; Gebala *et al.*, 2019; Konrad *et al.*, 2021).

Recipes

1. Deposition buffer
   200 mM NaCl + 10 mM TRIS, pH 7.6 – filtered.
   The concentration of salt can be varied: for example, we have obtained high-quality images at 200/50/10 mM NaCl or 50 mM NaCl + 2 mM $MgCl_2$, always in 10 mM TRIS, pH 7.6.

Acknowledgments

We thank Philipp Korber and Felix Müller-Planitz for help with initial nucleosome reconstitutions, Pauline Kolbeck, Tine Brouns, Wout Frederickx, Herlinde De Keersmaecker, Steven De Feyter, and Björn H. Menze for discussions and assistance with AFM imaging, and Thomas Nicolaus for help with sample preparation. This work was funded by the Deutsche Forschungsgemeinschaft (DFG, German Research Foundation) through SFB863 – Project ID 111166240. This protocol is based on our previously published study (Konrad *et al.*, 2021).

Competing interests

The authors declare no conflict of interest.

References

1. Ando, T. (2018). High-speed atomic force microscopy and its future prospects. *Biophys Rev* 10(2): 285-292.
2. Baldi, S., Korber, P. and Becker, P. B. (2020). Beads on a string-nucleosome array arrangements and folding of the chromatin fiber. *Nat Struct Mol Biol* 27(2): 109-118.
3. Bangalore, D. M., Heil, H. S., Mehringer, C. F., Hirsch, L., Hemmen, K., Heinze, K. G. and Tessmer, I. (2020). Automated AFM analysis of DNA bending reveals initial lesion sensing strategies of DNA glycosylases. *Sci Rep* 10(1): 15484.
4. Bintu, L., Kopaczynska, M., Hodges, C., Lubkowska, L., Kashlev, M. and Bustamante, C. (2011). The elongation rate of RNA polymerase determines the fate of transcribed nucleosomes. *Nat Struct Mol Biol* 18(12): 1394-1399.
5. Bowman, G. D. and Poirier, M. G. (2015). Post-translational modifications of histones that influence nucleosome dynamics. *Chem Rev* 115(6): 2274-2295.
6. Brouns, T., De Keersmaecker, H., Konrad, S. F., Kodera, N., Ando, T. and Lipfert, J. (2018). Free Energy Landscape and Dynamics of Supercoiled DNA by High-Speed Atomic Force Microscopy. *ACS Nano*12(12): 11907-11916.
7. Bussiek, M., Mücke, N., Langowski, J. (2003). Polylysine-coated mica can be used to observe systematic changes in the supercoiled DNA conformation by scanning force microscopy in solution. *Nucleic Acids Res* 31(22): e137.
8. Dufrêne, Y. F., Ando, T., Garcia, R., Alsteens, D., Martinez-Martin, D., Engel, A., Gerber, C. and Müller, D. J. (2017). Imaging modes of atomic force microscopy for application in molecular and cell biology. *Nat Nanotechnol* 12(4): 295-307.
9. Gebala, M., Johnson, S. L. and Narlikar, G. J. (2019). Ion counting demonstrates a high electrostatic field generated by the nucleosome. *eLife* 8: e44993.
10. Hall, M. A., Shundrovsky, A., Bai, L., Fulbright, R. M., Lis, J. T. and Wang, M. D. (2009). High-resolution dynamic mapping of histone-DNA interactions in a nucleosome. *Nat Struct Mol Biol* 16(2): 124-129.
11. Kaczmarczyk, A., Meng, H., Ordu, O. and Noort, J. V. (2020). Chromatin fibers stabilize nucleosomes under torsional stress. *Nat Commun* 11(1): 126.
12. Katan, A. J., Vlijm, R., Lusser, A. and Dekker, C. (2015). Dynamics of nucleosomal structures measured by high-speed atomic force microscopy. *Small* 11(8): 976-984.
13. Konrad, S. F., Vanderlinden, W., Frederickx, W., Brouns, T., Menze, B. H. and De Feyter, S. (2021). High-throughput AFM analysis reveals unwrapping pathways of H3 and CENP-A nucleosomes. *Nanoscale* 13(10): 5435-5447.
14. Krietenstein, N., Wippo, C. J., Lieleg, C. and Korber, P. (2012). Genome-wide *in vitro* reconstitution of yeast chromatin with *in vivo*-like nucleosome positioning. *Methods Enzymol* 513: 205-232.

15. Li, G. and Widom, J. (2004). Nucleosomes facilitate their own invasion. *Nat Struct Mol Biol* 11(8): 763-769.
16. Lipfert, J., Doniach, S., Das, R. and Herschlag, D. (2014). Understanding nucleic acid-ion interactions. *Annu Rev Biochem* 83: 813-841.
17. Luger, K., Mäder, A. W., Richmond, R. K., Sargent, D. F. and Richmond, T. J. (1997). Crystal structure of the nucleosome core particle at 2.8 A resolution. *Nature* 389(6648): 251-260.
18. Mihardja, S., Spakowitz, A. J., Zhang, Y. and Bustamante, C. (2006). Effect of force on mononucleosomal dynamics. *Proc Natl Acad Sci U S A* 103(43): 15871-15876.
19. Miyagi, A., Ando, T. and Lyubchenko, Y. L. (2011). Dynamics of nucleosomes assessed with time-lapse high-speed atomic force microscopy. *Biochemistry* 50(37): 7901-7908.
20. Mueller-Planitz, F., Klinker, H. and Becker, P. B. (2013). Nucleosome sliding mechanisms: new twists in a looped history. *Nat Struct Mol Biol* 20(9): 1026-1032.
21. Mullin, N. and Hobbs, J. K. (2014). A non-contact, thermal noise based method for the calibration of lateral deflection sensitivity in atomic force microscopy. *Rev Sci Instrum* 85(11): 113703.
22. Narlikar, G. J., Sundaramoorthy, R. and Owen-Hughes, T. (2013). Mechanisms and functions of ATP-dependent chromatin-remodeling enzymes. *Cell* 154(3): 490-503.
23. Ngo, T. T., Zhang, Q., Zhou, R., Yodh, J. G. and Ha, T. (2015). Asymmetric unwrapping of nucleosomes under tension directed by DNA local flexibility. *Cell* 160(6): 1135-1144.
24. Ordu, O., Lusser, A. and Dekker, N. H. (2016). Recent insights from *in vitro* single-molecule studies into nucleosome structure and dynamics. *Biophys Rev* 8(Suppl 1): 33-49.
25. Richmond, T. J. and Davey, C. A. (2003). The structure of DNA in the nucleosome core. *Nature* 423(6936): 145-150.
26. Sadakierska-Chudy, A. and Filip, M. (2015). A comprehensive view of the epigenetic landscape. Part II: Histone post-translational modification, nucleosome level, and chromatin regulation by ncRNAs. *Neurotox Res* 27(2): 172-197.
27. Schlingman, D. J., Mack, A. H., Kamenetska, M., Mochrie, S. G. J. and Regan, L. (2014). Routes to DNA accessibility: alternative pathways for nucleosome unwinding. *Biophys J* 107(2): 384-392.
28. Shlyakhtenko, L. S., Lushnikov, A. Y. and Lyubchenko, Y. L. (2009). Dynamics of nucleosomes revealed by time-lapse atomic force microscopy. *Biochemistry* 48(33): 7842-7848.
29. Sirinakis, G., Clapier, C. R., Gao, Y., Viswanathan, R., Cairns, B. R. and Zhang, Y. (2011). The RSC chromatin remodelling ATPase translocates DNA with high force and small step size. *Embo J* 30(12): 2364-2372.
30. van Noort, J., Orsini, F., Eker, A., Wyman, C., de Grooth, B. and Greve, J. (1999). DNA bending by photolyase in specific and non-specific complexes studied by atomic force microscopy. *Nucleic Acids Res* 27(19): 3875-3880.

31. Würtz, M., Aumiller, D., Gundelwein, L., Jung, P., Schütz, C., Lehmann, K., Tóth, K. and Rohr, K. (2019). DNA accessibility of chromatosomes quantified by automated image analysis of AFM data. *Sci Rep* 9(1): 12788.

